

Molecular and Clinical Relationship between Live-Attenuated Japanese Encephalitis Vaccination and Childhood Onset Myasthenia Gravis

Dan He, PhD,¹ Han Zhang, PhD,¹ Jun Xiao, PhD,¹ Xiaofan Zhang, PhD,¹ Minjie Xie, PhD,^{1,2} Dengji Pan, PhD,¹ Minghuan Wang, PhD,¹ Xiang Luo, PhD,¹ Bitao Bu, PhD,¹ Min Zhang, PhD,¹ and Wei Wang, PhD^{1,2}

Objective: The incidence of childhood onset myasthenia gravis (CMG) in China is higher than that in other countries; however, the reasons for this are unclear.

Methods: We investigated the clinical and immunological profiles of CMG, and assessed the potential precipitating factors. For the mouse studies, the possible implication of vaccination in the pathogenesis was explored.

Results: In our retrospective study, 51.22% of the 4,219 cases of myasthenia gravis (MG) were of the childhood onset type. The cohort study uncovered that the pathophysiology of CMG was mediated by immune deviation, rather than through gene mutations or virus infections. The administration of the live-attenuated Japanese encephalitis vaccine (LA-JEV), but not the inactivated vaccine or other vaccines, in mice induced serum acetylcholine receptor (AChR) antibody production, reduced the AChR density at the endplates, and decreased both muscle strength and response to repetitive nerve stimulation. We found a peptide (containing 7 amino acids) of LA-JEV similar to the AChR- α subunit, and immunization with a synthesized protein containing this peptide reproduced the MG-like phenotype in mice.

Interpretation: Our results describe the immunological profile of CMG. Immunization with LA-JEV induced an autoimmune reaction against the AChR through molecular mimicry. These findings might explain the higher occurrence rate of CMG in China, where children are routinely vaccinated with LA-JEV, compared with that in countries, where this vaccination is not as common. Efforts should be made to optimize immunization strategies and reduce the risk for developing autoimmune disorders among children.

ANN NEUROL 2018;84:386–400

Myasthenia gravis (MG) is an autoimmune disorder characterized by the loss of functional acetylcholine receptors (AChRs) from neuromuscular junctions (NMJs), mainly mediated by anti-AChR antibodies (AChRabs).¹ Childhood onset MG (CMG) is defined as MG with an age of onset < 15 years.^{2,3} Several reports have indicated regional variations in the proportion of CMG patients.⁴ According to a small cohort study we presented earlier, CMG comprises approximately 50% of all MG cases in

the Chinese mainland.³ In other populations, such as among people of European, American, Japanese, or Taiwanese origin, only 10 to 15% of patients with MG develop symptoms before they are 15 years old.^{5–10} These apparent discrepancies in the incidence rate imply that the underlying immunopathogenesis mechanisms may be different in different populations.

Although there have been no comprehensive studies investigating the correlation between human leukocyte

View this article online at wileyonlinelibrary.com. DOI: 10.1002/ana.25267

Received Sep 14, 2017, and in revised form May 22, 2018. Accepted for publication May 23, 2018.

Address correspondence to Dr W. Wang or Dr M. Zhang, Key Laboratory of Neurological Disease of Education Committee of China, Tongji Hospital, Tongji Medical College, Huazhong University of Science and Technology, 1095 Jiefang Road, Wuhan 430030, Hubei, China. E-mail: wwang@vip.126.com (W. Wang), mzhang@tjh.tjmu.edu.cn (M. Zhang).

D.H., H.Z., and J.X. contributed equally to this work.

From the ¹Department of Neurology, Tongji Hospital, Tongji Medical College, Huazhong University of Science and Technology; and ²Key Laboratory of Neurological Disease of Education Committee of China, Wuhan, Hubei, China

antigen (HLA) subtypes and CMG^{11–13} in Caucasians or Americans, HLA-DR9 and HLA-DQ9 haplotypes are suspected to carry a genetic risk for CMG in China²; similarly, HLA-DR9, HLA-DQ9, and HLA-DR13 are considered to be risk factors for CMG in Japan.^{14,15} In Taiwan and Hong Kong, HLA-Bw46 and HLA-DR9 haplotypes are positively associated with juvenile onset MG.^{16,17} Despite the similarity in genetic factors, the prevalence of CMG in these regions is different, suggesting that environmental factors might account for the regional differences in the onset-age distribution.¹⁸

The immune system undergoes different changes during the course of maturation from childhood to adulthood: The thymus cortex becomes thinner, and the number of naive T and B lymphocytes gradually decreases. Meanwhile, the serum concentration of immunoglobulins is lower during childhood than during adulthood.¹⁹ These characteristics make children vulnerable to viral infections. In adults, the involvement of viral infections in the etiology of MG remains controversial. Abnormal accumulation and activation of the Epstein–Barr virus (EBV) has been reported in the thymus of patients with MG, thus supporting the role of EBV infection in the initiation and development of adulthood onset MG.^{20,21} In China, however, recent reports have found no EBV infections in patients with adulthood onset MG.²² Whether EBV infection plays a role in CMG pathogenesis has not been demonstrated.

Another notable difference between children and adults lies in the frequency of vaccination. Vaccines have been implicated as a trigger of some immune diseases, including MG.^{23–25} Thirty-eight among the 2,161 CMG patients reported a history of inoculation before the onset, relapse, or exacerbation of MG symptoms. More importantly, > 40% of our patients with CMG presented with their first MG symptoms before they were 4 years of age, which coincides with the Chinese planned-immunization program timetable. This prompted us to explore the implication of vaccinations in the onset of CMG as well.

In this report, we studied 4,219 patients with MG to analyze the proportion of CMG. Then a cohort study was conducted to elucidate their immunological abnormalities and potential precipitating factors. Subsequent in-depth investigation was carried out in mice to explore the relationship between vaccination and the development of CMG.

Materials and Methods

Study Population and Procedures

Retrospective Analysis of Patients with MG. In the retrospective study, we analyzed the chart data from 4,219

consecutive outpatients diagnosed with MG, and followed them from January 1982 to July 2013 at Tongji Hospital in China. MG was diagnosed according to the standard criteria of the MG Foundation of America Clinical Classification.

Cohort Study of Patients with CMG. In the cohort study of the clinical and immunological features of CMG, we recruited 104 patients (from January 2011 to June 2013) with CMG, as well as 100 age- and sex-matched healthy controls. All the studies were approved by the institutional review board and local ethics committee, and informed consent was obtained from the parents of the participants. All the participants received vaccines included in the Chinese planned-immunization program (<http://www.nhfp.gov.cn/jnr/etyfjzssxx/201404/155e4191ce1548b7ba4e871a3594d998.shtml>). Blood samples were collected from the children when no active infections were reported. Subsequently, the serum titers of AChRAbs were estimated by enzyme-linked immunosorbent assay (ELISA; RSR, Cardiff, UK); titers > 0.45nM were considered positive.

Auxiliary Examinations. All patients in the cohort study received routine auxiliary examinations in the clinical laboratory, including (1) thyroid function tests, such as the free triiodothyronine, free thyroxine, thyroid-stimulating hormone, and antithyroglobulin antibody; (2) serum concentration of IgG, IgM, IgA, C3, and C4; (3) blood tests for evidence of common virus infections, including anti-cytomegalovirus/rubella virus/toxoplasma/herpes simplex virus (HSV) I/HSV II-IgM/IgG antibodies and anti-echovirus/human parvovirus B19/EBV/coxsackievirus-IgM; and (4) serum test for rheumatic disorders, such as rheumatoid factor, anticyclic citrullinated protein antibodies, double-stranded DNA, antinuclear antibodies.

Immunological Analyses. To analyze the changes in the immunological profiles, the serum concentration of Th1/Th2/Th9/Th17/Th22 cytokines were measured by the Human Th1/Th2/Th9/Th17/Th22 13plex FlowCytomix Kit (eBioscience, San Diego, CA) according to the manufacturer's instructions. This kit is a bead-based analyte detection system for quantitative detection of human IFN γ , IL1 β , IL2, IL4, IL5, IL6, IL9, IL10, IL12 p70, IL13, IL17A, IL22, and TNF α , by flow cytometry. To be specific, all the beads were coated with specific antibodies, and were differentiated by their sizes and their distinct spectral addresses. Then a mixture of coated beads and the sample were established, and the analytes presented in the sample would bind to the antibodies linked to the fluorescent beads. A biotin-conjugated second antibody was added, then streptavidin-phycoerythrin was also added to

bind to the biotin conjugate and emit fluorescent signals. Finally, these samples were analyzed by a flow cytometer, and the concentration of each cytokine was calculated by the eBioscience FlowCytomix software.

Meanwhile, the levels of serum IL23 and IL12/23 P40 were measured by the ELISA kits for quantitative detection of human IL23 (eBioscience) and IL12/23 P40 (R&D Systems, Minneapolis, MN) according to the manufacturers' instructions.

The thymus tissues were collected from 5 controls during corrective cardiovascular surgery and 5 patients with CMG after therapeutic thymectomy. Next, the thymus tissue samples were routinely prepared for staining with hematoxylin and eosin. Immunohistochemistry analysis was performed using antibodies against CD20 and CD21 (Abcam, Cambridge, UK). The EBV RNA encoding *EBER1* was probed by in situ hybridization using digoxigenin-labeled RNA probes in the thymus tissues.

Molecular Genetic Analysis. Fifteen patients with MG who were seronegative for AChRAb, 5 patients with MG who were seropositive for AChRAb, and 10 controls were screened for specific genetic mutations related to CMG. Genomic DNA was isolated from venous blood samples using a blood DNA extraction kit according to the manufacturer's recommendations (Qiagen, Hilden, Germany). The whole length of genes of *DOK7*, *RAPSN*, *CHRNE*, *COLQ*, *CHAT*, *CHRNA1*, *CHRND*, *CHRNA3*, *CHRNA4*, *CHRNA5*, *CHRNA7*, *CHRNA9*, *CHRNA10*, *CHRNA11*, *CHRNA12*, *CHRNA13*, *CHRNA14*, *CHRNA15*, *CHRNA16*, *CHRNA17*, *CHRNA18*, *CHRNA19*, *CHRNA20*, *CHRNA21*, *CHRNA22*, *CHRNA23*, *CHRNA24*, *CHRNA25*, *CHRNA26*, *CHRNA27*, *CHRNA28*, *CHRNA29*, *CHRNA30*, *CHRNA31*, *CHRNA32*, *CHRNA33*, *CHRNA34*, *CHRNA35*, *CHRNA36*, *CHRNA37*, *CHRNA38*, *CHRNA39*, *CHRNA40*, *CHRNA41*, *CHRNA42*, *CHRNA43*, *CHRNA44*, *CHRNA45*, *CHRNA46*, *CHRNA47*, *CHRNA48*, *CHRNA49*, *CHRNA50*, *CHRNA51*, *CHRNA52*, *CHRNA53*, *CHRNA54*, *CHRNA55*, *CHRNA56*, *CHRNA57*, *CHRNA58*, *CHRNA59*, *CHRNA60*, *CHRNA61*, *CHRNA62*, *CHRNA63*, *CHRNA64*, *CHRNA65*, *CHRNA66*, *CHRNA67*, *CHRNA68*, *CHRNA69*, *CHRNA70*, *CHRNA71*, *CHRNA72*, *CHRNA73*, *CHRNA74*, *CHRNA75*, *CHRNA76*, *CHRNA77*, *CHRNA78*, *CHRNA79*, *CHRNA80*, *CHRNA81*, *CHRNA82*, *CHRNA83*, *CHRNA84*, *CHRNA85*, *CHRNA86*, *CHRNA87*, *CHRNA88*, *CHRNA89*, *CHRNA90*, *CHRNA91*, *CHRNA92*, *CHRNA93*, *CHRNA94*, *CHRNA95*, *CHRNA96*, *CHRNA97*, *CHRNA98*, *CHRNA99*, *CHRNA100*, *CHRNA101*, *CHRNA102*, *CHRNA103*, *CHRNA104*, *CHRNA105*, *CHRNA106*, *CHRNA107*, *CHRNA108*, *CHRNA109*, *CHRNA110*, *CHRNA111*, *CHRNA112*, *CHRNA113*, *CHRNA114*, *CHRNA115*, *CHRNA116*, *CHRNA117*, *CHRNA118*, *CHRNA119*, *CHRNA120*, *CHRNA121*, *CHRNA122*, *CHRNA123*, *CHRNA124*, *CHRNA125*, *CHRNA126*, *CHRNA127*, *CHRNA128*, *CHRNA129*, *CHRNA130*, *CHRNA131*, *CHRNA132*, *CHRNA133*, *CHRNA134*, *CHRNA135*, *CHRNA136*, *CHRNA137*, *CHRNA138*, *CHRNA139*, *CHRNA140*, *CHRNA141*, *CHRNA142*, *CHRNA143*, *CHRNA144*, *CHRNA145*, *CHRNA146*, *CHRNA147*, *CHRNA148*, *CHRNA149*, *CHRNA150*, *CHRNA151*, *CHRNA152*, *CHRNA153*, *CHRNA154*, *CHRNA155*, *CHRNA156*, *CHRNA157*, *CHRNA158*, *CHRNA159*, *CHRNA160*, *CHRNA161*, *CHRNA162*, *CHRNA163*, *CHRNA164*, *CHRNA165*, *CHRNA166*, *CHRNA167*, *CHRNA168*, *CHRNA169*, *CHRNA170*, *CHRNA171*, *CHRNA172*, *CHRNA173*, *CHRNA174*, *CHRNA175*, *CHRNA176*, *CHRNA177*, *CHRNA178*, *CHRNA179*, *CHRNA180*, *CHRNA181*, *CHRNA182*, *CHRNA183*, *CHRNA184*, *CHRNA185*, *CHRNA186*, *CHRNA187*, *CHRNA188*, *CHRNA189*, *CHRNA190*, *CHRNA191*, *CHRNA192*, *CHRNA193*, *CHRNA194*, *CHRNA195*, *CHRNA196*, *CHRNA197*, *CHRNA198*, *CHRNA199*, *CHRNA200*, *CHRNA201*, *CHRNA202*, *CHRNA203*, *CHRNA204*, *CHRNA205*, *CHRNA206*, *CHRNA207*, *CHRNA208*, *CHRNA209*, *CHRNA210*, *CHRNA211*, *CHRNA212*, *CHRNA213*, *CHRNA214*, *CHRNA215*, *CHRNA216*, *CHRNA217*, *CHRNA218*, *CHRNA219*, *CHRNA220*, *CHRNA221*, *CHRNA222*, *CHRNA223*, *CHRNA224*, *CHRNA225*, *CHRNA226*, *CHRNA227*, *CHRNA228*, *CHRNA229*, *CHRNA230*, *CHRNA231*, *CHRNA232*, *CHRNA233*, *CHRNA234*, *CHRNA235*, *CHRNA236*, *CHRNA237*, *CHRNA238*, *CHRNA239*, *CHRNA240*, *CHRNA241*, *CHRNA242*, *CHRNA243*, *CHRNA244*, *CHRNA245*, *CHRNA246*, *CHRNA247*, *CHRNA248*, *CHRNA249*, *CHRNA250*, *CHRNA251*, *CHRNA252*, *CHRNA253*, *CHRNA254*, *CHRNA255*, *CHRNA256*, *CHRNA257*, *CHRNA258*, *CHRNA259*, *CHRNA260*, *CHRNA261*, *CHRNA262*, *CHRNA263*, *CHRNA264*, *CHRNA265*, *CHRNA266*, *CHRNA267*, *CHRNA268*, *CHRNA269*, *CHRNA270*, *CHRNA271*, *CHRNA272*, *CHRNA273*, *CHRNA274*, *CHRNA275*, *CHRNA276*, *CHRNA277*, *CHRNA278*, *CHRNA279*, *CHRNA280*, *CHRNA281*, *CHRNA282*, *CHRNA283*, *CHRNA284*, *CHRNA285*, *CHRNA286*, *CHRNA287*, *CHRNA288*, *CHRNA289*, *CHRNA290*, *CHRNA291*, *CHRNA292*, *CHRNA293*, *CHRNA294*, *CHRNA295*, *CHRNA296*, *CHRNA297*, *CHRNA298*, *CHRNA299*, *CHRNA300*, *CHRNA301*, *CHRNA302*, *CHRNA303*, *CHRNA304*, *CHRNA305*, *CHRNA306*, *CHRNA307*, *CHRNA308*, *CHRNA309*, *CHRNA310*, *CHRNA311*, *CHRNA312*, *CHRNA313*, *CHRNA314*, *CHRNA315*, *CHRNA316*, *CHRNA317*, *CHRNA318*, *CHRNA319*, *CHRNA320*, *CHRNA321*, *CHRNA322*, *CHRNA323*, *CHRNA324*, *CHRNA325*, *CHRNA326*, *CHRNA327*, *CHRNA328*, *CHRNA329*, *CHRNA330*, *CHRNA331*, *CHRNA332*, *CHRNA333*, *CHRNA334*, *CHRNA335*, *CHRNA336*, *CHRNA337*, *CHRNA338*, *CHRNA339*, *CHRNA340*, *CHRNA341*, *CHRNA342*, *CHRNA343*, *CHRNA344*, *CHRNA345*, *CHRNA346*, *CHRNA347*, *CHRNA348*, *CHRNA349*, *CHRNA350*, *CHRNA351*, *CHRNA352*, *CHRNA353*, *CHRNA354*, *CHRNA355*, *CHRNA356*, *CHRNA357*, *CHRNA358*, *CHRNA359*, *CHRNA360*, *CHRNA361*, *CHRNA362*, *CHRNA363*, *CHRNA364*, *CHRNA365*, *CHRNA366*, *CHRNA367*, *CHRNA368*, *CHRNA369*, *CHRNA370*, *CHRNA371*, *CHRNA372*, *CHRNA373*, *CHRNA374*, *CHRNA375*, *CHRNA376*, *CHRNA377*, *CHRNA378*, *CHRNA379*, *CHRNA380*, *CHRNA381*, *CHRNA382*, *CHRNA383*, *CHRNA384*, *CHRNA385*, *CHRNA386*, *CHRNA387*, *CHRNA388*, *CHRNA389*, *CHRNA390*, *CHRNA391*, *CHRNA392*, *CHRNA393*, *CHRNA394*, *CHRNA395*, *CHRNA396*, *CHRNA397*, *CHRNA398*, *CHRNA399*, *CHRNA400*, *CHRNA401*, *CHRNA402*, *CHRNA403*, *CHRNA404*, *CHRNA405*, *CHRNA406*, *CHRNA407*, *CHRNA408*, *CHRNA409*, *CHRNA410*, *CHRNA411*, *CHRNA412*, *CHRNA413*, *CHRNA414*, *CHRNA415*, *CHRNA416*, *CHRNA417*, *CHRNA418*, *CHRNA419*, *CHRNA420*, *CHRNA421*, *CHRNA422*, *CHRNA423*, *CHRNA424*, *CHRNA425*, *CHRNA426*, *CHRNA427*, *CHRNA428*, *CHRNA429*, *CHRNA430*, *CHRNA431*, *CHRNA432*, *CHRNA433*, *CHRNA434*, *CHRNA435*, *CHRNA436*, *CHRNA437*, *CHRNA438*, *CHRNA439*, *CHRNA440*, *CHRNA441*, *CHRNA442*, *CHRNA443*, *CHRNA444*, *CHRNA445*, *CHRNA446*, *CHRNA447*, *CHRNA448*, *CHRNA449*, *CHRNA450*, *CHRNA451*, *CHRNA452*, *CHRNA453*, *CHRNA454*, *CHRNA455*, *CHRNA456*, *CHRNA457*, *CHRNA458*, *CHRNA459*, *CHRNA460*, *CHRNA461*, *CHRNA462*, *CHRNA463*, *CHRNA464*, *CHRNA465*, *CHRNA466*, *CHRNA467*, *CHRNA468*, *CHRNA469*, *CHRNA470*, *CHRNA471*, *CHRNA472*, *CHRNA473*, *CHRNA474*, *CHRNA475*, *CHRNA476*, *CHRNA477*, *CHRNA478*, *CHRNA479*, *CHRNA480*, *CHRNA481*, *CHRNA482*, *CHRNA483*, *CHRNA484*, *CHRNA485*, *CHRNA486*, *CHRNA487*, *CHRNA488*, *CHRNA489*, *CHRNA490*, *CHRNA491*, *CHRNA492*, *CHRNA493*, *CHRNA494*, *CHRNA495*, *CHRNA496*, *CHRNA497*, *CHRNA498*, *CHRNA499*, *CHRNA500*, *CHRNA501*, *CHRNA502*, *CHRNA503*, *CHRNA504*, *CHRNA505*, *CHRNA506*, *CHRNA507*, *CHRNA508*, *CHRNA509*, *CHRNA510*, *CHRNA511*, *CHRNA512*, *CHRNA513*, *CHRNA514*, *CHRNA515*, *CHRNA516*, *CHRNA517*, *CHRNA518*, *CHRNA519*, *CHRNA520*, *CHRNA521*, *CHRNA522*, *CHRNA523*, *CHRNA524*, *CHRNA525*, *CHRNA526*, *CHRNA527*, *CHRNA528*, *CHRNA529*, *CHRNA530*, *CHRNA531*, *CHRNA532*, *CHRNA533*, *CHRNA534*, *CHRNA535*, *CHRNA536*, *CHRNA537*, *CHRNA538*, *CHRNA539*, *CHRNA540*, *CHRNA541*, *CHRNA542*, *CHRNA543*, *CHRNA544*, *CHRNA545*, *CHRNA546*, *CHRNA547*, *CHRNA548*, *CHRNA549*, *CHRNA550*, *CHRNA551*, *CHRNA552*, *CHRNA553*, *CHRNA554*, *CHRNA555*, *CHRNA556*, *CHRNA557*, *CHRNA558*, *CHRNA559*, *CHRNA560*, *CHRNA561*, *CHRNA562*, *CHRNA563*, *CHRNA564*, *CHRNA565*, *CHRNA566*, *CHRNA567*, *CHRNA568*, *CHRNA569*, *CHRNA570*, *CHRNA571*, *CHRNA572*, *CHRNA573*, *CHRNA574*, *CHRNA575*, *CHRNA576*, *CHRNA577*, *CHRNA578*, *CHRNA579*, *CHRNA580*, *CHRNA581*, *CHRNA582*, *CHRNA583*, *CHRNA584*, *CHRNA585*, *CHRNA586*, *CHRNA587*, *CHRNA588*, *CHRNA589*, *CHRNA590*, *CHRNA591*, *CHRNA592*, *CHRNA593*, *CHRNA594*, *CHRNA595*, *CHRNA596*, *CHRNA597*, *CHRNA598*, *CHRNA599*, *CHRNA600*, *CHRNA601*, *CHRNA602*, *CHRNA603*, *CHRNA604*, *CHRNA605*, *CHRNA606*, *CHRNA607*, *CHRNA608*, *CHRNA609*, *CHRNA610*, *CHRNA611*, *CHRNA612*, *CHRNA613*, *CHRNA614*, *CHRNA615*, *CHRNA616*, *CHRNA617*, *CHRNA618*, *CHRNA619*, *CHRNA620*, *CHRNA621*, *CHRNA622*, *CHRNA623*, *CHRNA624*, *CHRNA625*, *CHRNA626*, *CHRNA627*, *CHRNA628*, *CHRNA629*, *CHRNA630*, *CHRNA631*, *CHRNA632*, *CHRNA633*, *CHRNA634*, *CHRNA635*, *CHRNA636*, *CHRNA637*, *CHRNA638*, *CHRNA639*, *CHRNA640*, *CHRNA641*, *CHRNA642*, *CHRNA643*, *CHRNA644*, *CHRNA645*, *CHRNA646*, *CHRNA647*, *CHRNA648*, *CHRNA649*, *CHRNA650*, *CHRNA651*, *CHRNA652*, *CHRNA653*, *CHRNA654*, *CHRNA655*, *CHRNA656*, *CHRNA657*, *CHRNA658*, *CHRNA659*, *CHRNA660*, *CHRNA661*, *CHRNA662*, *CHRNA663*, *CHRNA664*, *CHRNA665*, *CHRNA666*, *CHRNA667*, *CHRNA668*, *CHRNA669*, *CHRNA670*, *CHRNA671*, *CHRNA672*, *CHRNA673*, *CHRNA674*, *CHRNA675*, *CHRNA676*, *CHRNA677*, *CHRNA678*, *CHRNA679*, *CHRNA680*, *CHRNA681*, *CHRNA682*, *CHRNA683*, *CHRNA684*, *CHRNA685*, *CHRNA686*, *CHRNA687*, *CHRNA688*, *CHRNA689*, *CHRNA690*, *CHRNA691*, *CHRNA692*, *CHRNA693*, *CHRNA694*, *CHRNA695*, *CHRNA696*, *CHRNA697*, *CHRNA698*, *CHRNA699*, *CHRNA700*, *CHRNA701*, *CHRNA702*, *CHRNA703*, *CHRNA704*, *CHRNA705*, *CHRNA706*, *CHRNA707*, *CHRNA708*, *CHRNA709*, *CHRNA710*, *CHRNA711*, *CHRNA712*, *CHRNA713*, *CHRNA714*, *CHRNA715*, *CHRNA716*, *CHRNA717*, *CHRNA718*, *CHRNA719*, *CHRNA720*, *CHRNA721*, *CHRNA722*, *CHRNA723*, *CHRNA724*, *CHRNA725*, *CHRNA726*, *CHRNA727*, *CHRNA728*, *CHRNA729*, *CHRNA730*, *CHRNA731*, *CHRNA732*, *CHRNA733*, *CHRNA734*, *CHRNA735*, *CHRNA736*, *CHRNA737*, *CHRNA738*, *CHRNA739*, *CHRNA740*, *CHRNA741*, *CHRNA742*, *CHRNA743*, *CHRNA744*, *CHRNA745*, *CHRNA746*, *CHRNA747*, *CHRNA748*, *CHRNA749*, *CHRNA750*, *CHRNA751*, *CHRNA752*, *CHRNA753*, *CHRNA754*, *CHRNA755*, *CHRNA756*, *CHRNA757*, *CHRNA758*, *CHRNA759*, *CHRNA760*, *CHRNA761*, *CHRNA762*, *CHRNA763*, *CHRNA764*, *CHRNA765*, *CHRNA766*, *CHRNA767*, *CHRNA768*, *CHRNA769*, *CHRNA770*, *CHRNA771*, *CHRNA772*, *CHRNA773*, *CHRNA774*, *CHRNA775*, *CHRNA776*, *CHRNA777*, *CHRNA778*, *CHRNA779*, *CHRNA780*, *CHRNA781*, *CHRNA782*, *CHRNA783*, *CHRNA784*, *CHRNA785*, *CHRNA786*, *CHRNA787*, *CHRNA788*, *CHRNA789*, *CHRNA790*, *CHRNA791*, *CHRNA792*, *CHRNA793*, *CHRNA794*, *CHRNA795*, *CHRNA796*, *CHRNA797*, *CHRNA798*, *CHRNA799*, *CHRNA800*, *CHRNA801*, *CHRNA802*, *CHRNA803*, *CHRNA804*, *CHRNA805*, *CHRNA806*, *CHRNA807*, *CHRNA808*, *CHRNA809*, *CHRNA810*, *CHRNA811*, *CHRNA812*, *CHRNA813*, *CHRNA814*, *CHRNA815*, *CHRNA816*, *CHRNA817*, *CHRNA818*, *CHRNA819*, *CHRNA820*, *CHRNA821*, *CHRNA822*, *CHRNA823*, *CHRNA824*, *CHRNA825*, *CHRNA826*, *CHRNA827*, *CHRNA828*, *CHRNA829*, *CHRNA830*, *CHRNA831*, *CHRNA832*, *CHRNA833*, *CHRNA834*, *CHRNA835*, *CHRNA836*, *CHRNA837*, *CHRNA838*, *CHRNA839*, *CHRNA840*, *CHRNA841*, *CHRNA842*, *CHRNA843*, *CHRNA844*, *CHRNA845*, *CHRNA846*, *CHRNA847*, *CHRNA848*, *CHRNA849*, *CHRNA850*, *CHRNA851*, *CHRNA852*, *CHRNA853*, *CHRNA854*, *CHRNA855*, *CHRNA856*, *CHRNA857*, *CHRNA858*, *CHRNA859*, *CHRNA860*, *CHRNA861*, *CHRNA862*, *CHRNA863*, *CHRNA864*, *CHRNA865*, *CHRNA866*, *CHRNA867*, *CHRNA868*, *CHRNA869*, *CHRNA870*, *CHRNA871*, *CHRNA872*, *CHRNA873*, *CHRNA874*, *CHRNA875*, *CHRNA876*, *CHRNA877*, *CHRNA878*, *CHRNA879*, *CHRNA880*, *CHRNA881*, *CHRNA882*, *CHRNA883*, *CHRNA884*, *CHRNA885*, *CHRNA886*, *CHRNA887*, *CHRNA888*, *CHRNA889*, *CHRNA890*, *CHRNA891*, *CHRNA892*, *CHRNA893*, *CHRNA894*, *CHRNA895*, *CHRNA896*, *CHRNA897*, *CHRNA898*, *CHRNA899*, *CHRNA900*, *CHRNA901*, *CHRNA902*, *CHRNA903*, *CHRNA904*, *CHRNA905*, *CHRNA906*, *CHRNA907*, *CHRNA908*, *CHRNA909*, *CHRNA910*, *CHRNA911*, *CHRNA912*, *CHRNA913*, *CHRNA914*, *CHRNA915*, *CHRNA916*, *CHRNA917*, *CHRNA918*, *CHRNA919*, *CHRNA920*, *CHRNA921*, *CHRNA922*, *CHRNA923*, *CHRNA924*, *CHRNA925*, *CHRNA926*, *CHRNA927*, *CHRNA928*, *CHRNA929*, *CHRNA930*, *CHRNA931*, *CHRNA932*, *CHRNA933*, *CHRNA934*, *CHRNA935*, *CHRNA936*, *CHRNA937*, *CHRNA938*, *CHRNA939*, *CHRNA940*, *CHRNA941*, *CHRNA942*, *CHRNA943*, *CHRNA944*, *CHRNA945*, *CHRNA946*, *CHRNA947*, *CHRNA948*, *CHRNA949*, *CHRNA950*, *CHRNA951*, *CHRNA952*, *CHRNA953*, *CHRNA954*, *CHRNA955*, *CHRNA956*, *CHRNA957*, *CHRNA958*, *CHRNA959*, *CHRNA960*, *CHRNA961*, *CHRNA962*, *CHRNA963*, *CHRNA964*, *CHRNA965*, *CHRNA966*, *CHRNA967*, *CHRNA968*, *CHRNA969*, *CHRNA970*, *CHRNA971*, *CHRNA972*, *CHRNA973*, *CHRNA974*, *CHRNA975*, *CHRNA976*, *CHRNA977*, *CHRNA978*, *CHRNA979*, *CHRNA980*, *CHRNA981*, *CHRNA982*, *CHRNA983*, *CHRNA984*, *CHRNA985*, *CHRNA986*, *CHRNA987*, *CHRNA988*, *CHRNA989*, *CHRNA990*, *CHRNA991*, *CHRNA992*, *CHRNA993*, *CHRNA994*, *CHRNA995*, *CHRNA996*, *CHRNA997*, *CHRNA998*, *CHRNA999*, *CHRNA1000*, *CHRNA1001*, *CHRNA1002*, *CHRNA1003*, *CHRNA1004*, *CHRNA1005*, *CHRNA1006*, *CHRNA1007*, *CHRNA1008*, *CHRNA1009*, *CHRNA1010*, *CHRNA1011*, *CHRNA1012*, *CHRNA1013*, *CHRNA1014*, *CHRNA1015*, *CHRNA1016*, *CHRNA1017*, *CHRNA1018*, *CHRNA1019*, *CHRNA1020*, *CHRNA1021*, *CHRNA1022*, *CHRNA1023*, *CHRNA1024*, *CHRNA1025*, *CHRNA1026*, *CHRNA1027*, *CHRNA1028*, *CHRNA1029*, *CHRNA1030*, *CHRNA1031*, *CHRNA1032*, *CHRNA1033*, *CHRNA1034*, *CHRNA1035*, *CHRNA1036*, *CHRNA1037*, *CHRNA1038*, *CHRNA1039*, *CHRNA1040*, *CHRNA1041*, *CHRNA1042*, *CHRNA1043*, *CHRNA1044*, *CHRNA1045*, *CHRNA1046*, *CHRNA1047*, *CHRNA1048*, *CHRNA1049*, *CHRNA1050*, *CHRNA1051*, *CHRNA1052*, *CHRNA1053*, *CHRNA1054*, *CHRNA1055*, *CHRNA1056*, *CHRNA1057*, *CHRNA1058*, *CHRNA1059*, *CHRNA1060*, *CHRNA1061*, *CHRNA1062*, *CHRNA1063*, *CHRNA1064*, *CHRNA1065*, *CHRNA1066*, *CHRNA1067*, *CHRNA1068*, *CHRNA1069*, *CHRNA1070*, *CHRNA1071*, *CHRNA1072*, *CHRNA1073*, *CHRNA1074*, *CHRNA1075*, *CHRNA1076*, *CHRNA1077*, *CHRNA1078*, *CHRNA1079*, *CHRNA1080*, *CHRNA1081*, *CHRNA108*

(OD) at 450nm was read using a microplate reader within 30 minutes.

Measurement of AChR Ab Serum Titers by RIA. RIA was performed according to the instructions of the RSR Acetylcholine Receptor Autoantibody RIA Kit. First, 15 μ l of sample sera (undiluted) was added to labeled assay tubes in duplicates. Next, 50 μ l of 125 I-AChR was added to each tube and the mixture was incubated overnight at 4 °C. The total counts were determined during this period and were subsequently probed with antimouse IgG overnight at 4 °C. Next, 25 μ l of precipitation enhancer was added to each tube (optional) and the mixture was washed twice. Finally, the incorporation of 125 I was recorded for 2 minutes by a gamma counter.

Measurement of the Reactivity between AChR Ab and JEV Antigen or RdRp by ELISA. A 96-well ELISA plate was coated with the culture supernatant of LA-JEV-transfected BHK-21 cells or recombinant RdRp protein diluted in carbonate/bicarbonate buffer (pH 9.6). Next, the plates were incubated at 4 °C overnight and blocked with 2% bovine serum albumin in PBS at room temperature for 30 minutes. The serum samples (1:100 dilution) from AChR-immunized mice were added and incubated at room temperature for 2 hours, following which 100 μ l HRP-conjugated goat antimouse IgG (Promoter) in the dilution buffer was added and incubated at room temperature for 90 minutes. Next, 100 μ l TMB solution was added and incubated for 15 minutes at room temperature. Finally, 100 μ l of 2M H_2SO_4 was added, and the OD at 450nm was read using a microplate reader within 30 minutes.

Measurement of Antineutrophil Cytoplasmic Antibody and MuSK-Ab Serum Titers. The serum concentration of antineutrophil cytoplasmic antibodies and MuSK-Abs was determined by the mouse perinuclear antineutrophil cytoplasmic antibody ELISA kit (Shguduo, Shanghai, China) and mouse MuSK-Ab ELISA kit (Jonln, Shanghai, China) according to the manufacturers' instructions.

Measurements of Muscle Strength. At week 8 of the experiment, the controls, LA-JEV-immunized animals, and RdRp-immunized animals were weighed and their limb motor activity was evaluated using the coat hanger test and a grip strength meter. For the coat hanger test, the mice were allowed to hang at the middle of a metal coat hanger with forepaws, observed for 2 minutes. The duration time of the mouse staying on the hanger was measured (hanging time). The mean value of 2 attempts was calculated for hanging time. For the grip strength measurement, mice were exercised by 30 paw grips on the cage top grid.

Following exercise, the grip strength was measured by a dynamometer (Chatillon Digital Force Gauge, DFE II; AMETEK, Largo, FL). The maximal force (T-peak) applied to the dynamometer was recorded while we pulled the mouse by its tail until release of paw grip from the grid. This measurement was repeated 5 times for each mouse.

Repetitive Nerve Stimulation. At week 8, the controls, LA-JEV-immunized mice, and RdRp-immunized mice were anesthetized. Ten repetitive stimuli were applied on the sciatic nerves with frequencies of 5Hz and 20Hz. A reduction in response was defined as a decrease of >10% of the fifth amplitude of the compound muscle action potential (CMAP), compared to the first response.³⁰ All the measurements were repeated twice and carried out by the same technician, who was blinded to the experimental grouping.

Analyses of AChRs at the NMJs. At week 8, mice from the control (n = 5), LA-JEV-immunized (n = 5), and RdRp-immunized (n = 5) groups were perfused with 2% glutaraldehyde and 4% paraformaldehyde. After washing by PBS, the cryosections were incubated with 5% bovine serum albumin in PBS at room temperature for 2 hours to block nonspecific antibody binding. Then the cryosections were incubated with alpha-bungarotoxin-biotin (1 μ g/ml; Invitrogen, Carlsbad, CA) for 3.5 hours at room temperature. The AChRs were visualized by successive incubation in avidin-fluorescein isothiocyanate (1:2,000; BD Biosciences, Franklin Lakes, NJ). The staining results were photographed with a fluorescence microscope (BX51; Olympus, Tokyo, Japan). To determine the structure and concentration changes of AChRs, the exposure time as well as other microscope settings were kept at a constant value. Pictures were analyzed using ImageJ software (National Institutes of Health, Bethesda, MD). Endplate areas were identified as clusters of AChRs. The fluorescence intensity of 135 to 169 endplates was recorded.

Preparation of Recombinant AChR, RdRp, and mtRdRp Proteins. The RdRp cDNA (forward primer: 5'-GAC-TAAGTATGAGGAAGATGTCAACC-3'; reverse primer: 5'-GGCCTTTATTTCCTGGATCAAGACGT-3') and AChR α 1-210 cDNA (forward primer: 5'-CCGGATCC-GAACATGAGACC-3'; reverse primer: 5'-CGGAATTC-CAGGCGCTGCATGAC-3') were obtained by reverse transcription polymerase chain reaction (PCR) from the LA-JEV and mouse muscle, respectively. The RdRp mutation gene was mutated from wild-type RdRp gene using recombinant PCR (round 1: forward primer 1: 5'-GAC-TAAGTATGAGGAAGATGTCAACC-3'; reverse primer 1: 5'-CCAGTAGCCTTCACCTCATAGCGGTATGGAT

GCTCAGGGTC-3'; round 2: forward primer 2: 5'-GACCCTGAGCATCCATACCGCTATGAAGTGAAGGCTACTGG-3'; reverse primer 2: 5'-GGCCTTTATTCC TGGATCAAGACGT-3'; round 3: forward primer 3: 5'-GACTAAGTATGAGGAAGATGTCAACC-3'; reverse primer 3: 5'-GGCCTTTATTCCCTGGATCAAGACGT-3'). Then the genes encoding RdRp and mtRdRp were cloned in the pET28a-SUMO expression vector, whereas the gene encoding AChR α 1-210 was cloned in the pET32a expression vector. The vectors were expressed in the *Escherichia coli* Rosetta expression system (Novagen, Madison, WI). The recombinant proteins were cleaved by a proteinase, and purified by metal chelated affinity chromatography on Ni²⁺ nitriloacetic acid agarose. In addition, as shown in Figure 7, these recombinant proteins have been analyzed on sodium dodecyl sulfate–polyacrylamide gel electrophoresis gel for purity and size confirmation.

Sequence Analyses and 3-Dimensional Modeling. The amino acid sequences of the AChR- α subunit (human and murine) and LA-JEV were obtained from the PubMed website, and compared using Basic Local Alignment Search Tool (BLAST). A 3-dimensional model of the crystal structure of the AChR- α subunit was obtained from Structure (a molecular modeling database). A 3-dimensional model of RdRp was obtained using 3D-JIGSAW software (<http://bmm.crick.ac.uk/~3djigsaw/>) and visualized using PyMOL software (<https://pymol.org/2/>).

Dot blot. First, 2.5 μ l of antigens (100 μ g/ml of ovalbumin [OVA]/TWTYDGS peptide conjugated to OVA [Pep + OVA]/RdRp) were spotted on to a piece of nitrocellulose membrane. After blocking nonspecific binding sites with 5% nonfat milk and 0.25% Tween-20 (Amresco, Solon, OH) in Tris-buffered saline for 1 hour at room temperature, the membranes were incubated with target serum (1:20 diluted) at 4 °C on a rocker platform overnight. Then, the membranes were washed and incubated with the appropriate antimouse or antihuman HRP-conjugated secondary antibodies (1:5,000; Santa Cruz Biotechnology, Santa Cruz, CA). Finally, membranes were detected by an enhanced chemiluminescence kit (Thermo Fisher Scientific, Waltham, MA) according to the manufacturer's protocol.

Statistical Analysis

The results are presented as mean \pm standard error of mean. The statistical analyses were performed with the unpaired *t* test, 1-way analysis of variance, or Mantel–Haenszel chi-squared test using SPSS version 16.0 (SPSS, Chicago, IL). Results with *p* values < 0.05 were considered statistically significant.

Results

Clinical Features and Immunological Profiles of Patients

Clinical Characteristics of CMG in China. In the retrospective analysis, the basic data of 4,219 MG patients were included. Among them, a total of 2,161 patients (51.22%) developed MG before 15 years of age (Table 1), and were termed as CMG. Approximately 89.17% of the patients with CMG (1,927 patients) presented with isolated oculomotor symptoms within 2 years of onset. Strikingly, 936 of these patients (43.31% of all the CMG cases) first presented with the MG symptoms when they were younger than 4 years.

Immunological Features of Patients with CMG. To determine the clinical and immunological features of CMG, we performed a cohort study, recruiting 104 patients with CMG and 100 age- and sex-matched healthy controls. The age of onset of CMG ranged from 1 month to 15 years, with a mean of 5 years 4 months. Seventy-two of 104 patients (69.2%) were positive for AChRabs, with titers between 0.45 and 172 nM (Fig 1A).

TABLE 1. Clinical Characteristics of 2,161 Patients with Childhood Onset Myasthenia Gravis in the Retrospective Study

| Characteristics | Patients, n (%) | F/M |
|------------------------|-----------------|---------|
| Age at onset | | |
| 0–4 years | 936 (43.31) | 524/412 |
| 4–14 years | 1,225 (56.69) | 576/649 |
| Osserman criteria | | |
| I | 1,927 (89.17) | 978/949 |
| IIa | 125 (5.78) | 66/59 |
| IIb | 94 (4.35) | 51/43 |
| III | 11 (0.51) | 2/9 |
| IV | 4 (0.19) | 3/1 |
| Thymus abnormality | | |
| Thymoma | 48 (2.22) | 22/26 |
| Hyperplasia | 254 (11.75) | 139/115 |
| Normal | 1,859 (86.02) | 982/877 |
| Thymectomized patients | 45 (2.08) | 22/23 |
| Hyperthyroidism | 94 (4.35) | 50/44 |

F, female; M, male.

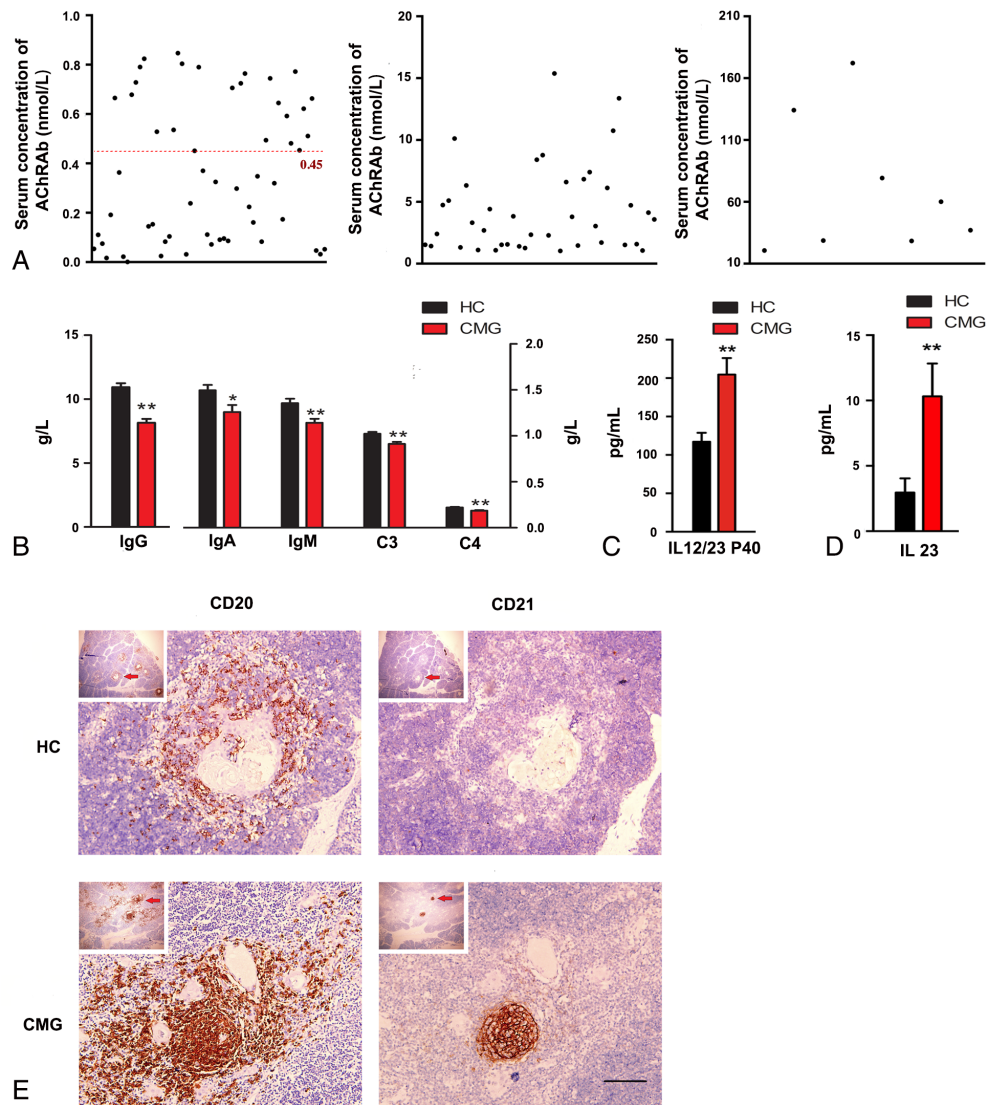


FIGURE 1: Clinical and immunological profiles of patients with childhood onset myasthenia gravis (CMG). (A) Serum concentration of anti-acetylcholine receptor antibodies (AChRABs) in the CMG patients of our cohort study. Serum titers > 0.45nM were considered positive (red line; n = 104). (B) Serum concentration of IgG, IgM, IgA, C3, and C4 in CMG patients (red columns; n = 104) is significantly lower than that in healthy controls (HC; black columns; n = 100,); * $p < 0.05$, ** $p < 0.01$. (C) Serum concentration of IL12/23 P40 in CMG patients (red column; n = 104) is significantly higher than that in HC (black column; n = 100); ** $p < 0.01$. (D) Serum concentration of IL23 in CMG patients (red column; n = 104) is significantly higher in patients than in HC (black column; n = 100); ** $p < 0.01$. (E) Representative images of the thymus in patients with CMG and HC. The CD20⁺ and CD21⁺ B cells aggregate to form a germinal center in the thymic medulla. Higher magnification images of the areas indicated by the arrows are shown. Scale bar = 25 μ m.

We also assayed the concentration of IgG, IgM, IgA, C3, and C4 in the serum of the patients by ELISA (see Fig 1). Compared with the normal controls, the CMG patients had lower concentration of IgG (8.15 ± 0.31 vs 10.95 ± 0.30 g/l for healthy controls, $p < 0.01$), IgA (1.26 ± 0.08 vs 1.50 ± 0.06 g/l for healthy controls, $p < 0.05$), IgM (1.14 ± 0.04 vs 1.36 ± 0.05 g/l for healthy controls, $p < 0.01$), C3 (0.91 ± 0.02 vs 1.02 ± 0.02 g/l for healthy controls, $p < 0.01$), and C4 (0.19 ± 0.01 vs 0.22 ± 0.01 g/l for healthy controls, $p < 0.01$). Cytokine levels in the sera of patients with CMG and healthy controls in our cohort were then assessed to test the

involvement of Th cells in the pathogenesis of CMG. The concentrations of IFN γ , IL1 β , IL2, IL4, IL5, IL6, IL9, IL10, IL12 p70, IL13, IL17A, IL22, and TNF α did not significantly differ between patients with CMG and healthy controls. However, the concentrations of IL12/23 P40 (CMG, 204.71 ± 21.48 pg/ml; controls, 117.19 ± 11.76 pg/ml; $p = 0.001$) and IL23 (CMG, 10.32 ± 2.51 pg/ml; controls, 2.96 ± 1.08 pg/ml; $p = 0.009$) were higher in patients than in controls.

Another prominent feature of autoimmune MG is abnormalities in the thymus.²¹ The pathological study revealed infiltration of CD20⁺ B cells and formation of

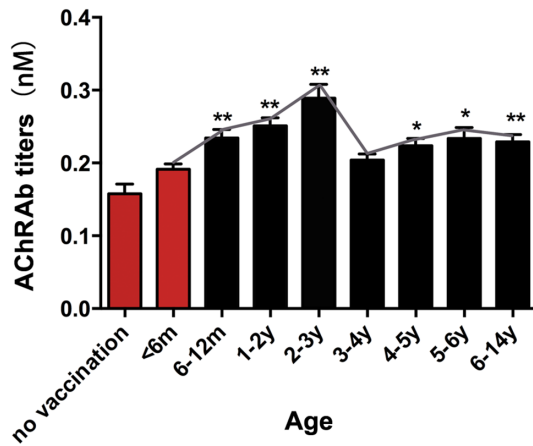


FIGURE 3: Serological features of children immunized with live-attenuated Japanese encephalitis vaccine (LA-JEV). Serum anti-acetylcholine receptor antibody (AChRab) titers in children vaccinated with LA-JEV at different ages are shown. The red columns represent serum titers in children who were not inoculated with LA-JEV (m = months; y = years; * $p < 0.05$, ** $p < 0.01$). For the no vaccination group, children did not receive any vaccine, including LA-JEV.

The possible implication of vaccinations in the development of MG drew our attention, because vaccines have been reported to induce immune diseases, including MG. Among the 2,161 CMG patients, 38 patients reported or were reported to have been immunized before the onset, relapse, or exacerbation of MG symptoms, prompting us to explore the implication of vaccinations in the onset of CMG in China.

LA-JEV Immunization Induces Features of MG

We injected BALB/c mice with a group of vaccines required by the Chinese planned-immunization program, including LA-JEV, DTaP, MMR, HBV, and BCG, as well as IA-JEV, adjuvants, and PBS.

Serologic Features of Mice. In the pilot study, we only observed an increase in the AChRab levels of mice injected with 1 dose of LA-JEV (1/5 of the human dose) twice or 4 times, and 5 doses of LA-JEV twice (data not shown). Therefore, we injected mice with 5 doses of LA-JEV ($5.7 \log_{10}$ PFU) 4 times, or the other vaccines, and measured the serum levels of AChRabs by both ELISA and RIA. We observed significantly higher mean AChRab levels in mice injected with LA-JEV than in PBS-injected controls, but not in those injected with other vaccines, including the IA-JEV, or adjuvants (thimerosal and aluminum hydroxide; Fig 2). We also analyzed some other antibodies, such as antineutrophil cytoplasmic antibodies and MuSK-Abs to avoid nonspecific binding, and these antibodies showed no differences among groups (data not shown). To confirm the cross-reactivity between LA-JEV

and AChR, culture supernatants of BHK-21 cells infected with LA-JEV were tested for reactivity with AChRabs. We found that the supernatants bound to the sera of mice immunized with *Torpedo californica*-derived AChRs, but not to those of mice immunized with PBS.

Serologic Features of Children. To clarify the relationship between LA-JEV immunization and AChRabs production, we assayed AChRab titers in healthy children without known autoimmune or infectious diseases. According to the Chinese planned-immunization program, children are inoculated with LA-JEV at 6 months and 2 years of age. Notably, the serum AChRab titers began to increase after inoculation at 6 months, reached a maximum around 2 years, and decreased slightly thereafter (Fig 3; $n = 40$ per group). In comparison, titers in 11 children who were not inoculated with LA-JEV did not increase. We also assayed some other pathogenic autoantibodies, such as antithyroglobulin antibodies and MuSK-Abs, and found no age-related change (data not shown). Taken together, this distinct pattern of changes in AChRab titers fits with the timing of LA-JEV immunization in children, suggesting a possible role for LA-JEV vaccination in the production of AChRabs.

MG-like Manifestations in Mice Immunized by LA-JEV.

In addition to the higher levels of AChRabs, significantly compromised motor activity as evaluated by a grip strength meter and the coat hanger test was detected in mice injected with LA-JEV (5 doses 4 times), but not in mice injected with PBS (Fig 4A, B). No change in body weight was noted in mice injected with LA-JEV or PBS. Moreover, at week 8 after immunization, repetitive nerve stimulation demonstrated a decrease of $>10\%$ in the CMAP in 4 of 19 and 3 of 19 LA-JEV mice at 20Hz and 5Hz, respectively, but no decrease in the CMAP in the PBS-injected controls (see Fig 4C, D). The mean percentage decrease in the CMAP at 20Hz was $8.53 \pm 3.56\%$ in mice injected with LA-JEV, significantly greater than that in mice injected with PBS ($0.9 \pm 0.76\%$; $p < 0.05$).

To further investigate the effects of LA-JEV immunization on the density and distribution of AChR at NMJs, the left tibial anterior muscles of the mice were isolated, sectioned, and stained for AChRs by immunofluorescence in the 8th week after inoculation. As shown in Figure 4, densely packed clusters of AChRs (green) were easily identified at the endplates in the mice injected with PBS, but were barely discernible in part of NMJ of the mice injected with LA-JEV. Quantitative analysis revealed that the fluorescence intensity of the AChR per NMJ in the LA-JEV-injected mice was significantly lower than that in the control mice ($p < 0.01$).

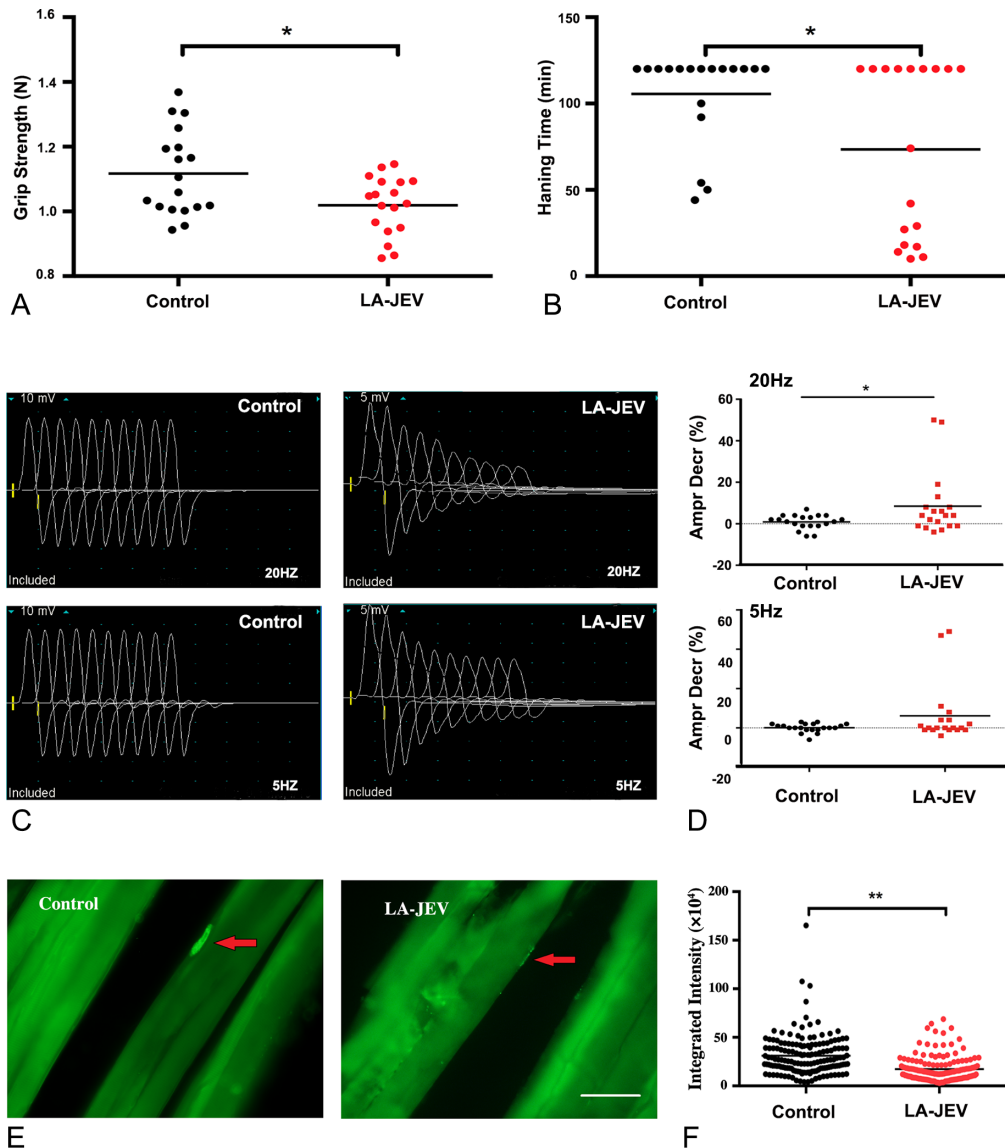


FIGURE 4: Mice injected with live-attenuated Japanese encephalitis vaccine (LA-JEV) develop features of myasthenia gravis. BALB/c mice were given intraperitoneal injections of 5.7 log₁₀ plaque-forming units/time LA-JEV or phosphate-buffered saline (PBS; control) 4 times at 2-week intervals. (A) The grip strength of control and LA-JEV-immunized mice, and (B) the lengths of time for which the LA-JEV-injected and control mice were able to hang from a coat hanger were tested at week 8. Mice vaccinated with LA-JEV had significantly reduced grip strength and hanging time when compared with the mice injected with the PBS control (**p* < 0.05; red dots). (C) Representative image of the compound muscle action potential (CMAP) responses in control and LA-JEV-injected mice at 8 weeks after first injection upon repetitive nerve stimulation. Mice injected with LA-JEV had a decreased CMAP response compared to the control mice. (D) When 20Hz stimulation was administered, the percentage decrease in CMAPs was significantly greater in mice injected with LA-JEV than in control mice (**p* < 0.05; *n* = 20 for the control group; *n* = 19 for the LA-JEV group, upper panel). Five-hertz stimulation did not induce a statistically significant reduction in the CMAP response between the control and LA-JEV-injected mice (lower panel). Ampr Decr % denotes the percentage decrease in the 5th amplitude of the CMAP compared to the first response. (E) Representative image of the immunofluorescence staining of acetylcholine receptors (AChRs) with biotin-conjugated α -bungarotoxin in muscle sections derived from mice injected with PBS (control) or LA-JEV. In the control mice, AChRs (labeled by green fluorescence) aggregated at the endplates (red arrows), whereas in LA-JEV-immunized mice, AChR staining was faint (scale bar = 25 μ m). (F) The mean fluorescence intensity of AChRs randomly selected from 169 neuromuscular junctions of 5 mice injected with LA-JEV (red) was significantly lower than that of control mice (black; ***p* < 0.01).

RdRp Recapitulates MG-like Manifestations

To elucidate the mechanism underlying the cross-reactivity between LA-JEV and AChR, the sequences of LA-JEV (SA-14-14-2) and the AChR- α subunit (both human and murine) were compared using the BLAST. An

86% (6/7) identity was confirmed in a 7-amino-acid-long region shared by both the extracellular fragment in the human/murine AChR α -subunit (TWTYDGS) and RdRp (TWTYHGS), which belongs to the C-terminal of NS5, and is generated during the replication of LA-JEV in vivo

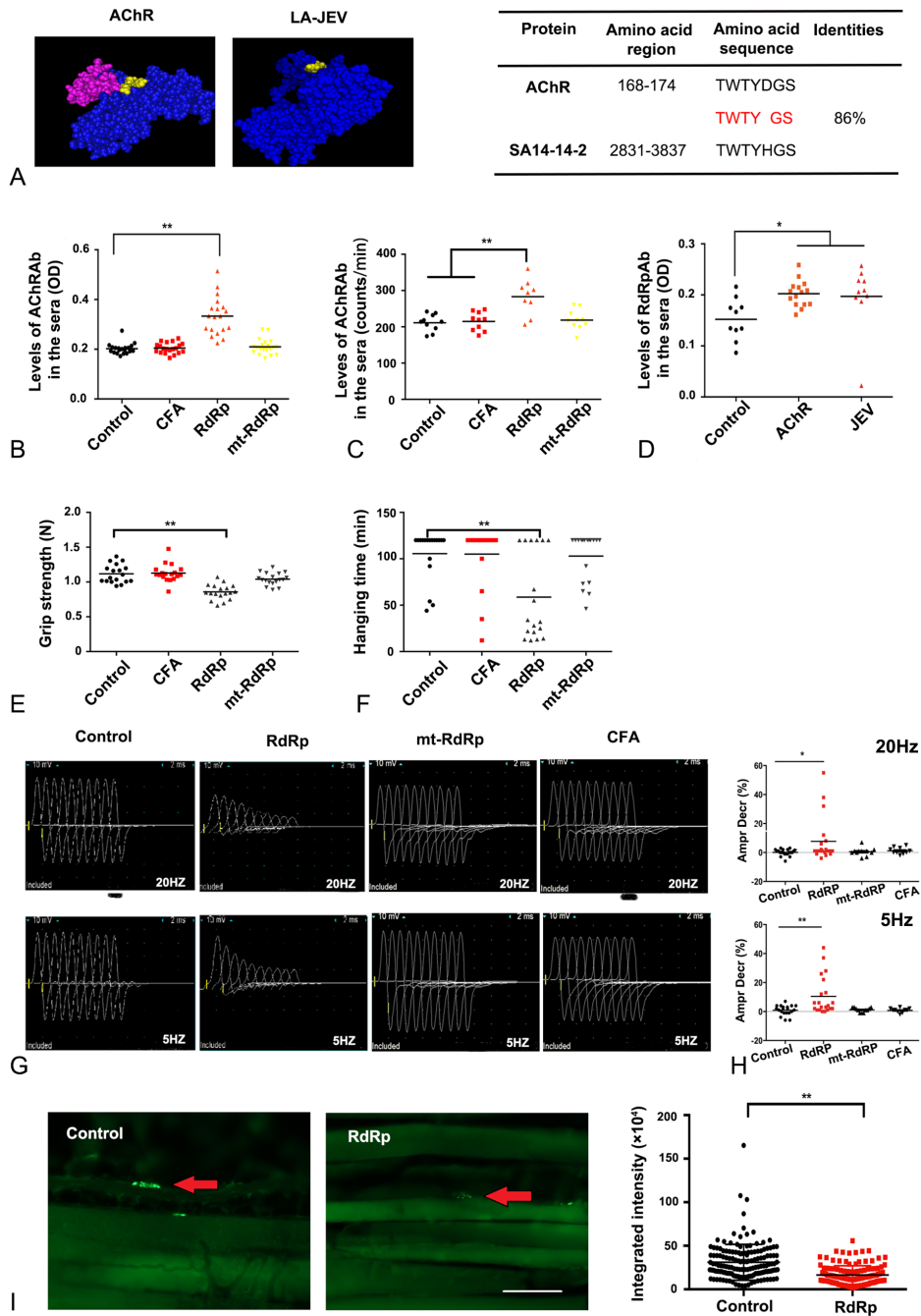


FIGURE 5: RdRp induces a myasthenia gravis-like phenotype through molecular mimicry. (A) Structures of the 2 proteins, acetylcholine receptor (AChR) and RNA-dependent RNA polymerase (RdRp; left panel). The highlighted regions indicate the 7-amino-acid-long region that is 86% identical between AChR and live-attenuated Japanese encephalitis vaccine (LA-JEV), based on Basic Local Alignment Search Tool analysis. The table on the right shows the sequences of this region in the 2 proteins. (B) The serum concentration of AChR antibodies (AChRABs) in mice injected 4 times at 2-week intervals with RdRp (orange), mutated (mt-RdRp) (yellow), complete Freund adjuvant (CFA; red), and phosphate-buffered saline (PBS; control), as measured by enzyme-linked immunosorbent assay (***p* < 0.01, *n* = 20). Mice injected with RdRp produced a significantly higher mean level of AChRABs than mice injected with PBS. (C) The serum concentration of AChRABs in mice injected 4 times at 2-week intervals with RdRp (orange), mtRdRp (yellow), CFA (red), and PBS (control), as measured by radioimmunoassay (***p* < 0.01). (D) AChRAB induced by torpedo AChR reacted strongly to RdRp protein (**p* < 0.05). (E) The grip strength and (F) the duration of hanging of control (PBS)-, CFA-, RdRp-, and mtRdRp-immunized mice as tested at week 8. The grip strength and hanging time were lower in mice injected with RdRp compared to the control mice (***p* < 0.01), whereas the mtRdRp- and CFA-immunized groups were not significantly different in their mean grip strength and hanging time. (G) Representative image of the compound muscle action potential (CMAP) responses in control, CFA-, RdRp-, and mtRdRp-injected mice at 8 weeks after first injection upon repetitive nerve stimulation. Mice injected with RdRp showed a decreased CMAP response 8 weeks after the first injection, whereas the mtRdRp- and CFA-immunized groups did not. (H) Compared with the control mice, the percentage reduction in CMAPs after the

(Fig 5).³⁴ Theoretically, antibodies against RdRp might cross-react with the AChR to induce autoimmunity. Then we injected BALB/c mice with either RdRp, mtRdRp that did not contain the said 7-amino-acid region, adjuvant (CFA), or PBS. Using both ELISA and RIA, significantly higher levels of AChRABs were detected in mice injected with RdRp, but not in those injected with mutated RdRp or CFA. Similarly, AChRABs also reacted with the RdRp antigen *in vitro*. An MG-like phenotype evaluated by motor activity tests and repetitive nerve stimulation (both at 20Hz and 5Hz) was found in mice injected with RdRp, but not in the mice immunized with CFA, mtRdRp, or PBS. Similarly, the fluorescence intensity of AChRs per NMJ was 47.04% lower in mice immunized with RdRp than that in controls ($p < 0.001$).

To further evaluate whether the said 7-amino-acid region is the antigenic epitope, we further evaluated the cross-reactivity between the serum of LA-JEV/RdRp-immunized mice and the TWTYDGS epitope (Fig 6A). As expected, the serum from LA-JEV/RdRp-immunized mice could react with TWTYDGS epitope. Then, we also determined the concentrations at which the postvaccination cross-reaction would occur. In Figure 6B, TWTYHGS epitope could be displaced by TWTYDGS epitope over the concentration of 3.13 $\mu\text{g/ml}$.

Finally, we investigated the cross-reactivity of the serum from CMG patients, adult MG patients, and healthy children with this TWTYDGS epitope. As is seen in Figure 6C, the serum of CMG patients containing the AChR autoantibodies reacted with the TWTYDGS epitope (the AChR of mice and human has the same epitope), indicating this epitope is one of the antigenic epitopes that may cause MG-like manifestation for CMG patients. However, for most of the adulthood onset MG patients, the serum did not show reaction with the TWTYDGS epitope, suggesting a different pathogenesis when compared with CMG. We further calculated the proportion of positive cross-reaction between epitope TWTYDGS and the serum of CMG and adulthood onset MG patients. For CMG patients, the serum of 70% patients reacted with the TWTYDGS epitope. For the adulthood onset MG patients, the serum of 30% patients reacted with the TWTYDGS epitope (data not shown).

Taken together, all these observations suggest that vaccination with LA-JEV induced the production of antibodies against the RdRp. The anti-RdRp antibodies interacted with AChRs on the endplates; thus, the integrity and function of the AChR were compromised, thereby generating the symptoms of MG.

Discussion

To investigate the incidence of CMG, we first retrospectively analyzed the chart data of 4,219 MG patients at Tongji Hospital, which represents the largest survey of MG performed in the Chinese population so far.^{3,35} Our data disclosed that CMG accounted for >50% of MG cases with a mean onset age of 5.36 years, and the exceptionally high percentage of CMG cases reported only in the mainland of China prompted us to further explore the pathogenesis underlying CMG.

The cohort study systemically described the clinical profile of CMG, including the serum titer of AChRABs, and changes in the immunoglobulin and complement, thymus, and Th cell function. These characteristics distinguish the CMG patients from other autoimmune disease. For the most likely factors responsible for the high percentage of Chinese CMG, our preliminary data did not indicate the involvement of viral infections, gene mutations, or other types of autoimmune diseases in the pathogenesis of CMG. Vaccines have been proposed to induce immune disorders.^{24,25} That > 40% of the patients with CMG presented with their first symptoms before 4 years of age (this phenomenon has not been previously described in detail in other cohort studies), in keeping with the timetable of the Chinese planned-immunization program, implied that vaccination might trigger the onset of CMG in China.

Studies involving both human subjects and rats have shown the immunopathogenic mechanisms of MG, including antigenic modulation by AChRABs, complement-mediated destruction of the postsynaptic membrane, and competitive inhibition of the AChRAB-AChR binding.^{36,37} To investigate the possible role of vaccination in CMG pathogenesis, we injected BALB/c mice with a group of vaccines administered as part of the Chinese planned-immunization program. Among all the vaccines we tested,

mice were injected with RdRp was significant greater upon 20Hz (upper panel) and 5Hz (lower panel) stimulation, whereas the mtRdRp- and CFA-immunized groups showed no difference. Ampr Decr % denotes the percentage decrease in the 5th amplitude of the CMAP compared to the first response (* $p < 0.05$, ** $p < 0.01$). (I) Representative image (left panel) of the immunofluorescence staining of AChRs with biotin-conjugated α -bungarotoxin in muscle sections derived from mice injected with PBS (control) or RdRp. In control mice, AChRs (labeled by green fluorescence) aggregated in the endplates (red arrows), whereas in mice injected with RdRp, AChR staining was barely detected (scale bar = 25 μm). In the right panel, the fluorescence intensity of AChRs at 135 neuromuscular junctions from 5 randomly selected mice injected with RdRp (red) were significantly lower than that of AChRs selected from control mice (black), ** $p < 0.01$. OD = optical density.

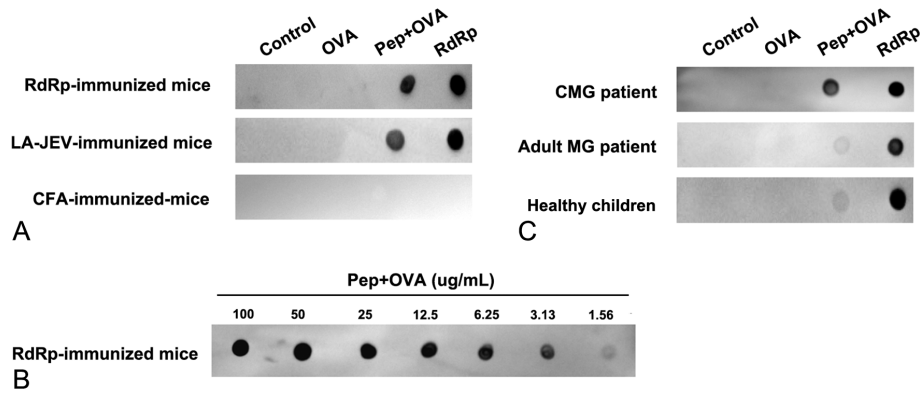


FIGURE 6: Injection with live-attenuated Japanese encephalitis vaccine (LA-JEV) leads to the production of anti-acetylcholine receptor antibodies (AChRabs). (A) The reactivity of the serum from LA-JEV/RNA-dependent RNA polymerase (RdRp)/complete Freund adjuvant (CFA)-immunized mice with the TWTYDGS epitope was tested by dot blot. LA-JEV/RdRp-immunized mouse serum could react with TWTYDGS conjugated to ovalbumin (Pep+OVA). (B) The samples of Pep+OVA were 2-fold serial diluted and spotted onto a piece of nitrocellulose membrane. RdRp-immunized mouse serum could react with Pep+OVA at a concentration of 3.13 $\mu\text{g/ml}$. (C) The serum of childhood onset myasthenia gravis (CMG) patients could react with the TWTYDGS epitope, whereas that of adult myasthenia gravis (MG) patients and healthy controls were less likely to react with the TWTYDGS epitope. OVA = ovalbumin.

only LA-JEV showed a cross-reactivity with the AChR. Accordingly, we also monitored the focal lysis of AChRs on the postsynaptic membrane as well as the impairment of nerve conduction at the NMJ. More interestingly, the increase in AChRab concentrations after Japanese encephalitis (JE) vaccination has also been observed in children, which might play a role in initiating the pathogenic cascade of MG in both human subjects and mice models.

The sequences of LA-JEV (SA-14-14-2) and AChR- α subunit (both human and murine) were compared using BLAST, which revealed a 7-amino-acid sequence that shared 86% identity between AChR and RdRp; both these sequences appear to be on the surface and are, therefore, accessible to antibodies *in vivo*. Thus, antibodies against RdRp might cross-react with AChR to induce autoantibodies that lead to MG. This speculation was substantiated by an LA-JEV-like AChRab response elicited in

mice by RdRp injection. Furthermore, our results demonstrated that the TWTYDGS epitope was responsible for the cross-reactivity for both mouse and CMG. Overall, our findings suggest that LA-JEV immunization triggers the clinical and pathophysiological changes characteristic of human MG in mice.

JE is an endemic disease in Asia and the Western Pacific, and is caused by the JE virus. Approximately 35,000 to 50,000 JE cases were reported annually before JE vaccination began, and the estimated mortality has reached 30%.³⁸⁻⁴¹ As no effective therapy is currently available, JE vaccination became the mandatory method to prevent JE in Asian countries. There are 2 types of JEV in use, namely IA-JEV and LA-JEV. Given the economic concerns, long-term immunity, and a simpler immunization strategy, LA-JEV is widely used in China, Thailand, Sri Lanka, Nepal, India, and Cambodia,⁴²⁻⁴⁸ which

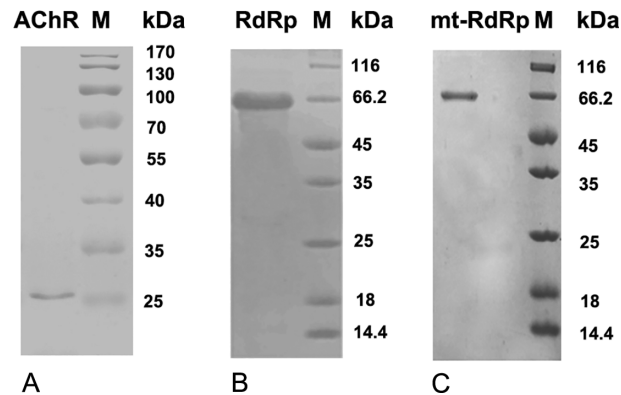


FIGURE 7: Representative band patterns of the recombinant proteins after sodium dodecyl sulfate-polyacrylamide gel electrophoresis (SDS-PAGE). Purified proteins were electrophoresed by 12% SDS-PAGE and stained with Coomassie Brilliant Blue R250. (A) acetylcholine receptor (AChR)- α 1-210, (B) RNA-dependent RNA polymerase (RdRp), and (C) mutated (mt)-RdRp were detected as 25, 66.2, and 66.2kDa bands.

comprise about one-third of the world's population. Moreover, the LA-JEV has been accepted and enrolled in the World Health Organization purchase catalogue. In the mainland of China, LA-JEV has been used to immunize approximately 20 to 30 million children every year.⁴⁶ In contrast, in Japan and Taiwan, only IA-JEV has been approved in the expanded immunization program.^{49–51} Although cumulative research indicates that LA-JEV has an acceptable safety profile,^{43,46} the live attenuated vaccine carries some risk of adverse events.^{52,53} In Europe, North America, and Australia,^{40,50} JEV is not included in the national immunization programs because JE cases are rarely reported in these regions. If our results are correct, the limited use of LA-JEV might explain why the incidence of CMG is low in these areas of the world.

Vaccination is one of the most effective ways to combat infectious diseases. However, problems generated by immunization, such as vaccination-related Guillain-Barré syndrome, narcolepsy, acute disseminating encephalomyelitis, and multiple sclerosis, are becoming a public concern.^{23,47,54–61} Whether the cellular and humoral autoimmunity related to LA-JEV vaccination is involved in other immune-mediated neurological diseases also remains unclear.

Although our research has provided numerous lines of evidence that suggest a link among vaccination, autoimmunity, and development of CMG, there are limitations to this study. The AChRab levels were only modestly raised, but similar levels were reported in other experimental studies⁶² and our experimental autoimmune MG models. We also measured the AChRab titer of our CMG patients, as mapped in Figure 1A. Sixty-eight percent of CMG patients had a titer < 1 nmol/l, whereas only 25.33% patient had a titer range from 1 to 10 nmol/l, and 3.33% patients had a titer > 10 nmol/l. This phenomenon could also be found in patients in whom much of the antibody is bound to the motor endplates.⁶³ However, the molecular mechanisms involved in NMJ pathology⁶⁴ caused by the relatively lower antibody levels still remain to be clarified. Moreover, additional factors such as the associated HLA haplotype or different immunological profiles would be expected to develop clinical features of the disease. Future prospective studies are needed to study the incidence of CMG and its relationship with LA-JEV vaccination. If confirmed, efforts should be made to optimize immunization strategies and reduce the risk of autoimmune disorders among children.

Acknowledgment

This work was supported by grants from the Natural Science Foundation of China (81571113, 61327902, and

81271406) and Huazhong University of Science and Technology “Double Top” Construction Project of International Cooperation (540-5001540013).

We thank the patients who participated in the study; Drs W. Zou and A. Vincent for advice regarding the immunological study of Chinese CMG; and Dr B. R. Ransom for discussions regarding the construction of this article.

Author Contributions

D.H., H.Z., J.X., X.Z., M.X., M.W., X.L., D.P., B.B., M.Z., and W.W. were responsible for designing and performing the experiments; D.H., H.Z., J.X., and M.Z. were responsible for acquiring and analyzing the data; D.H., B.B., M.Z., and W.W. were responsible for drafting the manuscript and figures. All the authors reviewed, revised, and approved the final manuscript.

Potential Conflicts of Interest

Nothing to report.

References

- Meriglioli MN, Sanders DB. Autoimmune myasthenia gravis: emerging clinical and biological heterogeneity. *Lancet Neurol* 2009;8:475–490.
- Zhu WH, Lu JH, Lin J, et al. HLA-DQA1*03:02/DQB1*03:03:02 is strongly associated with susceptibility to childhood-onset ocular myasthenia gravis in Southern Han Chinese. *J Neuroimmunol* 2012;247:81–85.
- Zhang X, Yang M, Xu J, et al. Clinical and serological study of myasthenia gravis in HuBei Province, China. *J Neurol Neurosurg Psychiatry* 2007;78:386–390.
- Carr AS, Cardwell CR, McCarron PO, McConville J. A systematic review of population based epidemiological studies in myasthenia gravis. *BMC Neurol* 2010;10:46.
- Lai CH, Tseng HF. Nationwide population-based epidemiological study of myasthenia gravis in Taiwan. *Neuroepidemiology* 2010;35:66–71.
- Murai H, Yamashita N, Watanabe M, et al. Characteristics of myasthenia gravis according to onset-age: Japanese nationwide survey. *J Neurol Sci* 2011;305:97–102.
- Alshekhlee A, Miles JD, Katirji B, et al. Incidence and mortality rates of myasthenia gravis and myasthenic crisis in US hospitals. *Neurology* 2009;72:1548–1554.
- Aguilar Ade A, Carvalho AF, Costa CM, et al. Myasthenia gravis in Ceara, Brazil: clinical and epidemiological aspects. *Arq Neuropsiquiatr* 2010;68:843–848.
- Ashraf VV, Taly AB, Veerendrakumar M, Rao S. Myasthenia gravis in children: a longitudinal study. *Acta Neurol Scand* 2006;114:119–123.
- Finnis MF, Jayawant S. Juvenile myasthenia gravis: a paediatric perspective. *Autoimmune Dis* 2011;2011:404101.
- Compston DA, Vincent A, Newsom-Davis J, Batchelor JR. Clinical, pathological, HLA antigen and immunological evidence for disease heterogeneity in myasthenia gravis. *Brain* 1980;103:579–601.

12. Fang F, Sveinsson O, Thormar G, et al. The autoimmune spectrum of myasthenia gravis: a Swedish population-based study. *J Intern Med* 2015;277:594–604.
13. Deitiker PR, Oshima M, Smith RG, et al. Association with HLA DQ of early onset myasthenia gravis in Southeast Texas region of the United States. *Int J Immunogenet* 2011;38:55–62.
14. Matsuki K, Juji T, Tokunaga K, et al. HLA antigens in Japanese patients with myasthenia gravis. *J Clin Invest* 1990;86:392–399.
15. Shinomiya N, Nomura Y, Segawa M. A variant of childhood-onset myasthenia gravis: HLA typing and clinical characteristics in Japan. *Clin Immunol* 2004;110:154–158.
16. Chen WH, Chiu HC, Hsieh RP. Association of HLA-Bw46DR9 combination with juvenile myasthenia gravis in Chinese. *J Neurol Neurosurg Psychiatry* 1993;56:382–385.
17. Hawkins BR, Ip MS, Lam KS, et al. HLA antigens and acetylcholine receptor antibody in the subclassification of myasthenia gravis in Hong Kong Chinese. *J Neurol Neurosurg Psychiatry* 1986;49:316–319.
18. Evoli A. Acquired myasthenia gravis in childhood. *Curr Opin Neurol* 2010;23:536–540.
19. McDade TW. Life history, maintenance, and the early origins of immune function. *Am J Hum Biol* 2005;17:81–94.
20. Cavalcante P, Maggi L, Colleoni L, et al. Inflammation and Epstein-Barr virus infection are common features of myasthenia gravis thymus: possible roles in pathogenesis. *Autoimmune Dis* 2011;2011:213092.
21. Cavalcante P, Serafini B, Rosicarelli B, et al. Epstein-Barr virus persistence and reactivation in myasthenia gravis thymus. *Ann Neurol* 2010;67:726–738.
22. Jing F, Wei D, Wang D, et al. Lack of Epstein-Barr virus infection in Chinese myasthenia gravis patients. *Acta Neurol Scand* 2013;128:345–350.
23. Stubgen JP. Neuromuscular disorders associated with Hepatitis B vaccination. *J Neurol Sci* 2010;292:1–4.
24. Molina V, Shoenfeld Y. Infection, vaccines and other environmental triggers of autoimmunity. *Autoimmunity* 2005;38:235–245.
25. Nachamkin I, Shadomy SV, Moran AP, et al. Anti-ganglioside antibody induction by swine (A/NJ/1976/H1N1) and other influenza vaccines: insights into vaccine-associated Guillain-Barre syndrome. *J Infect Dis* 2008;198:226–233.
26. Huzé C, Bauché S, Richard P, et al. Identification of an agrin mutation that causes congenital myasthenia and affects synapse function. *Am J Hum Genet* 2009;85:155–167.
27. Maselli RA, Ng JJ, Anderson JA, et al. Mutations in LAMB2 causing a severe form of synaptic congenital myasthenic syndrome. *J Med Genet* 2009;46:203–208.
28. Selcen D, Juel VC, Hobson-Webb LD, et al. Myasthenic syndrome caused by plectinopathy. *Neurology* 2011;76:327–336.
29. Wargon I, Richard P, Kuntzer T, et al. Long-term follow-up of patients with congenital myasthenic syndrome caused by COLQ mutations. *Neuromuscul Disord* 2012;22:318–324.
30. Losen M, Stassen MH, Martínez-Martínez P, et al. Increased expression of rapsyn in muscles prevents acetylcholine receptor loss in experimental autoimmune myasthenia gravis. *Brain* 2005;128(pt 10):2327–2337.
31. Cufi P, Dragin N, Weiss JM, et al. Implication of double-stranded RNA signaling in the etiology of autoimmune myasthenia gravis. *Ann Neurol* 2013;73:281–293.
32. Gowing EC, McKown KM. Myasthenia gravis in a patient with pauciarticular juvenile chronic arthritis. *J Clin Rheumatol* 2002;8:269–272.
33. Man BL, Mok CC, Fu YP. Neuro-ophthalmologic manifestations of systemic lupus erythematosus: a systematic review. *Int J Rheum Dis* 2014;17:494–501.
34. Wang Q, Weng L, Tian X, et al. Effect of the methyltransferase domain of Japanese encephalitis virus NS5 on the polymerase activity. *Biochim Biophys Acta* 2012;1819:411–418.
35. Wang W, Chen YP, Wang ZK, et al. A cohort study on myasthenia gravis patients in China. *Neurol Sci* 2013;34:1759–1764.
36. Drachman DB, Kao L, Angus CW, Murphy A. Effect of myasthenic immunoglobulin on ACh receptors of cultured muscle. *Trans Am Neurol Assoc* 1977;102:96–100.
37. Howard FM Jr, Lennon VA, Finley J, et al. Clinical correlations of antibodies that bind, block, or modulate human acetylcholine receptors in myasthenia gravis. *Ann N Y Acad Sci* 1987;505:526–538.
38. Mackenzie JS, Gubler DJ, Petersen LR. Emerging flaviviruses: the spread and resurgence of Japanese encephalitis, West Nile and dengue viruses. *Nat Med* 2004;10(12 suppl):S98–S109.
39. Erlanger TE, Weiss S, Keiser J, et al. Past, present, and future of Japanese encephalitis. *Emerg Infect Dis* 2009;15:1–7.
40. Fischer M, Lindsey N, Staples JE, et al. Japanese encephalitis vaccines: recommendations of the Advisory Committee on Immunization Practices (ACIP). *MMWR Recomm Rep* 2010;59:1–27.
41. Mackenzie JS, Smith DW. Japanese encephalitis virus: geographic distribution, incidence, and spread of a virus with a propensity to emerge in new areas. *Pers Med Virol* 2006;16:201–268.
42. Yang D, Li XF, Ye Q, et al. Characterization of live-attenuated Japanese encephalitis vaccine virus SA14-14-2. *Vaccine* 2014;32:2675–2681.
43. Wijesinghe PR, Abeysinghe MR, Yoksan S, et al. Safety and immunogenicity of live-attenuated Japanese encephalitis SA 14-14-2 vaccine co-administered with measles vaccine in 9-month-old infants in Sri Lanka. *Vaccine* 2014;32:4751–4757.
44. Wang HJ, Li XF, Ye Q, et al. Recombinant chimeric Japanese encephalitis virus/tick-borne encephalitis virus is attenuated and protective in mice. *Vaccine* 2014;32:949–956.
45. Kumar R, Tripathi P, Rizvi A. Effectiveness of one dose of SA 14-14-2 vaccine against Japanese encephalitis. *N Engl J Med* 2009;360:1465–1466.
46. Liu Y, Lin H, Zhu Q, et al. Safety of Japanese encephalitis live attenuated vaccination in post-marketing surveillance in Guangdong, China, 2005-2012. *Vaccine* 2014;32:1768–1773.
47. Japanese encephalitis: status of surveillance and immunization in Asia and the Western Pacific, 2012. *Wkly Epidemiol Rec* 2013;88:357–364.
48. Liu W, Clemens JD, Yang JY, Xu ZY. Immunization against Japanese encephalitis in China: a policy analysis. *Vaccine* 2006;24:5178–5182.
49. Huang LM, Lin TY, Chiu CH, et al. Concomitant administration of live attenuated Japanese encephalitis chimeric virus vaccine (JE-CV) and measles, mumps, rubella (MMR) vaccine: randomized study in toddlers in Taiwan. *Vaccine* 2014;32:5363–5369.
50. Trent DW, Minor P, Jivapaisarnpong T, et al. WHO working group on the quality, safety and efficacy of Japanese encephalitis vaccines (live attenuated) for human use, Bangkok, Thailand, 21-23 February 2012. *Biologicals* 2013;41:450–457.
51. Appaiahgari MB, Vrti S. IMOJEV(®): a yellow fever virus-based novel Japanese encephalitis vaccine. *Expert Rev Vaccines* 2010;9:1371–1384.
52. Rowhani-Rahbar A, Fireman B, Lewis E, et al. Effect of age on the risk of fever and seizures following immunization with measles-containing vaccines in children. *JAMA Pediatr* 2013;167:1111–1117.
53. Samtivilai S, Xiang Z, Shedden KA, et al. Ontology-based combinatorial comparative analysis of adverse events associated with killed and live influenza vaccines. *PLoS One* 2012;7:e49941.

54. Romio S, Weibel D, Dieleman JP, et al. Guillain-Barre syndrome and adjuvanted pandemic influenza A (H1N1) 2009 vaccines: a multinational self-controlled case series in Europe. *PLoS One* 2014;9:e82222.
55. Sipilä JO, Soilu-Hänninen M. The incidence and triggers of adult-onset Guillain-Barré syndrome in southwestern Finland 2004-2013. *Eur J Neurol* 2015;22:292-298.
56. Karussis D, Petrou P. The spectrum of post-vaccination inflammatory CNS demyelinating syndromes. *Autoimmun Rev* 2014;13:215-224.
57. Langer-Gould A, Qian L, Tartof SY, et al. Vaccines and the risk of multiple sclerosis and other central nervous system demyelinating diseases. *JAMA Neurol* 2014;71:1506-1513.
58. Pellegrino P, Carnovale C, Perrone V, et al. Acute disseminated encephalomyelitis onset: evaluation based on vaccine adverse events reporting systems. *PLoS One* 2013;8:e77766.
59. Nohynek H, Jokinen J, Partinen M, et al. AS03 adjuvanted AH1N1 vaccine associated with an abrupt increase in the incidence of childhood narcolepsy in Finland. *PLoS One* 2012;7:e33536.
60. Partinen M, Saarenpää-Heikkilä O, Ilveskoski I, et al. Increased incidence and clinical picture of childhood narcolepsy following the 2009 H1N1 pandemic vaccination campaign in Finland. *PLoS One* 2012;7:e33723.
61. Sarkanen TO, Alakujala APE, Dauvilliers YA, Partinen MM. Incidence of narcolepsy after H1N1 influenza and vaccinations: systematic review and meta-analysis. *Sleep Med Rev* 2018;38:177-186.
62. Aissaoui A, Klingel-Schmitt I, Couderc J, et al. Prevention of autoimmune attack by targeting specific T-cell receptors in a severe combined immunodeficiency mouse model of myasthenia gravis. *Ann Neurol* 1999;46:559-567.
63. Leite MI, Jacob S, Viegas S, et al. IgG1 antibodies to acetylcholine receptors in 'seronegative' myasthenia gravis. *Brain* 2008;131(pt 7):1940-1952.
64. Maurer M, Bougoin S, Feferman T, et al. IL-6 and Akt are involved in muscular pathogenesis in myasthenia gravis. *Acta Neuropathol Commun* 2015;3:1.